Fast kinetic spectroscopy, decoloration and production of H_2O_2 induced by visible light in oxygenated solutions of the azo dye Orange II

Jayasundera Bandara and John Kiwi*

Institute of Physical Chemistry II, Swiss Federal Institute of Technology, Lausanne 1015, Switzerland. E-mail: John.Kiwi@epfl.ch

Received* (*in Montpellier, France*) *24th March 1999, Accepted 21st April 1999

A fast kinetics study by pulsed laser spectroscopy allows a mechanism for Orange II photobleaching in the presence of O_2 to be proposed. Evidence is presented that the hydroperoxy radical $HO_2^{\cdot}$ is the main oxidative species for Orange II in oxygenated aqueous solution under visible light irradiation. The probability of reaction between O_2 and Orange II leading to radical formation ($\approx 5 \times 10^{-4}$) is observed to be very low. The lifetime and amplitude of the radicals anions and cations in solution are compared in O_2-, air- and Ar-containing solutions. Singlet oxygen ($^1O_2$) is shown not to be present during the initial photobleaching stages of Orange II. Steady-state irradiation of Orange II in aqueous solution in the presence of O_2 causes two simultaneous processes: photodegradation to more biodegradable intermediates with CO_2 evolution and photoinduced generation of peroxides in solution. The observed peroxide generation stops when initial Orange II reaches a low concentration and does not occur from the intermediates during the photodegradation of Orange II. Direct electron transfer from excited Orange II to O_2 provides the driving force for the accelerated photodegradation of the dye. No electron transfer to O_2 was observed in the dark involving the ground state of the azo dye. The oxidation potential Orange II/Orange$^{+\cdot}$ is determined by cyclic voltammetry to be 0.76 V(NHE) and a value of -1.54 V(NHE) could be estimated for the oxidation potential of the couple Orange II*/Orange$^{+\cdot}$.

Azo dyes are biorecalcitrant compounds found in common industrial effluents in a wide concentration range.[1–3] Traditional non-destructive treatment methods like filtration, reverse osmosis and flocculation have been used to abate this type of pollutant.[2–4] However, these treatment methods are expensive. An energetically less demanding approach using mild conditions to decolorize the azo dye Orange II is the object of this study, using visible light to photobleach the dye in oxygenated solutions. Until now only a few studies have been reported on the photobleaching of dyes such as fluorescein,[4] porphyrins,[5,6] crystal violet[7] and J-aggregates of a few azo dyes[8] and these studies have had some application in tumor photochemotherapy.[6]

This study focuses on the decoloration of the azo dye Orange II in oxygenated solutions under light. The fast kinetics spectra are examined with the aim of identifying the transient kinetics of the intermediates participating in the decoloration process. The steady-state processes involved in the degradation, decoloration and photoproduct formation are dealt with in the later part of this work. Commercial textile azo dyes like Acid Orange 7[9] and Orange II (the Na salt of Acid Orange 7) are both stable to photobleaching. In Orange II the *ortho*-OH substitution stabilizes the dye because of strong internal bond formation and tautomerism, which inhibits ionization, hydrogen abstraction and *cis-trans* isomerization. The ability of Fenton systems to photodegrade Orange II,[9–14] a nonbiodegradable textile azo dye, is of recent interest. It is an important part of the work in the area of photo-oxidative degradation of water pollutants.[15]

The present study addresses the role and limits of O_2 under light as an oxidant in place of the Fenton photo-assisted reaction. We set out to investigate the parameters affecting the photobleaching of Orange II in oxygenated solution with the objective of understanding the kinetics, mechanism and intermediates involved in the photochemical decoloration by pulsed laser spectroscopy. The approach presented is of interest as a pretreatment method for the subsequent biological degradation of non-biodegradable azo dyes.

Experimental

Materials

Orange II is 4-(2-hydroxy-1-naphthyl)azobenzene sulfonic acid. This reagent and NaN_3 were Fluka p.a. grade and were used as received. DABCO (2,1,4-diazabicyclo[2,2,2]octane) was obtained from Aldrich (p.a., 99.5%). The value for the molar absorption coefficient of Orange II was found to be 17,330 mol^{-1} cm^{-1} at $\lambda = 490$ nm. Tri-distilled water from a Millipore-Q water purification system was used throughout this study. The formula of Orange II is shown below.

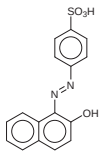

Photoreactor and procedures

Photolysis was carried out inside the cavity of a Hanau Suntest solar simulator with a radiant flux of 80 mW cm^{-2} and provided with air cooling regulated at $\approx 35\,^{\circ}C$. The lamp had a wavelength distribution with about 7% of the emitted photons between 290 and 400 nm. The profile of the photons emitted between 400 to 800 nm followed the sun spectrum.

The photochemical irradiation vessels used were 60 mL cylindrical Pyrex flasks (cutoff $\lambda = 330$ nm), each containing 40 mL of solution. The radiant flux in integrated mW cm^{-2} was measured with a Yellow Springs photometer (Yellow Springs, Co, USA). Spectrophotometric analyses of the solutions used were followed *via* a Hewlett–Packard 8452 diode array spectrophotometer.

Laser flash photolysis

Laser photolysis was carried out by using the second harmonic ($\lambda = 347$ nm) of a JK-2000 ruby laser operated in the Q-switched mode.[12] A routine optical T-scheme was used with (*a*) Xe monitoring lamp, (*b*) sample cell between two condensed lenses, (*c*) monochromator and (*d*) photomultiplier. The laser excitation beam was perpendicular to the monitoring light. The Xe monitoring light reaching the cell was filtered at the appropriate wavelength with SKF filters positioned between the lamp and the cell. For each wavelength, the appropriate Schott SKF passband filter was selected. These filters had a bandpass width of $\Delta\lambda = 20$ nm and were centered at the λ of interest. All experiments have been performed in 1 cm quartz cells in aerated solutions at room temperature. The pulse width was about 15 ns and the energy per pulse was ≈ 10 mJ. The laser pulse energy was monitored and the experimental results normalized according to these measured energies. The mean average of the laser beam diameter was 0.5 cm.

Analyses in solution and techniques employed

Spectrophotometric analyses of the solutions used were carried out *via* a Hewlett–Packard 8452 diode array spectrophotometer. The total organic carbon (TOC) was monitored by a Shimadzu 500 instrument equipped with an automatic sample injector. Detection of CO_2 was performed with a Carlo Erba GC unit equipped with a thermal conductivity detector using a Poropak Q column. He was used as a carrier gas. The O_2 content of the solution was monitored with a YSI Model 5300 probe (Clark electrode).

An HPLC (Varian 9065 Diode Array) was used for identification of reaction intermediates in solution. For Orange II a Phenomenex C-18 inverse phase column was employed and the signals for the dye were detected at 282 nm with a retention time of 20.1 min. The solution gradient was regulated with a buffer consisting of ammonium acetate and methanol. The peaks observed for the reaction intermediates were referenced with appropriate external standards. Quantification of the peaks in the HPLC spectrograms was based on the integrated band component of each compound. Analysis of oxalic acid was carried out by means of an H-801 column (Interaction) in isocratic mode at 60 °C. The eluant was H_2SO_4 (0.01 N). For the analysis of other organic intermediates (see Scheme 1 below) an ODS-2 column was employed. The eluant was a mixture of ammonium acetate (0.03 M) and acetonitrile.

The presence of nitrates, nitrites and sulfates was verified by ion liquid chromatography (ICL) with a Dionex DX-100 ion analyzer. The column employed was a Dionex Ion Pac-As 14 M with a mobile phase consisting of 3.5 mM Na_2CO_3 and 1.5 mM $NaHCO_3$ at pH 5.5. Ammonia was also detected by a Tecator instrument after sample aliquots were injected into a NaOH–borax mixture. The resulting color change was monitored at $\lambda = 590$ nm.

The oxidation potential of Orange II was determined in an Autolab 20 cyclic voltammeter, *vs.* Ag/AgCl in 0.1 M $HClO_4$ solution. The working electrode was of glassy carbon. A carbon counter-electrode was employed during cyclic voltammetry.

For the BOD_5 measurements, a bacterial solution (inoculum) was taken after the primary decantation at the biological waste water treatment station of Vidy (VD, Switzerland). The solution was further decanted 24 h, filtered through cotton and used as inoculum in the laboratory experiments. A blank BOD_5 reference run was referenced using only bacteria.

BOD_5 (biological oxygen demand in a 5-day period) measurements have been carried out in an Oxytop WTW 1230 Hg-free unit using a 20% inoculum in a solution containing phosphate buffer and the necessary nutrient salts and trace elements.[13]

Inductively coupled plasma spectroscopy (ICPS) was carried out to analyze the traces of iron in solution with a Hewlett Packard 20 M instrument.

Results and discussion

Nature of the oxidative intermediates during Orange II photobleaching under steady-state irradiation

The reduction of an initial Orange II concentration of 0.32 mM at pH 3 is shown in Fig. 1(A) and at pH 6 in Fig. 1(B) when NaN_3 was added (traces 1) and when this reagent was absent from solution (traces 2). In both cases the decrease in the initial concentration of the dye is modest in the presence and absence of NaN_3 during the first $\approx$5–6 h. The NaN_3 affects the Orange II degradation at longer times when Orange II has already been degraded to a considerable extent into more oxidizable intermediates. At the beginning when Orange II is the only light absorber in solution, the added NaN_3 has little effect on the Orange II disappearance, indicating that $^1O_2$ is not involved during the initial stages of the reaction. Only when intermediates have been generated in solution to a significant amount, are they in a position to interact with $^1O_2$ under light irradiation. The decoloration with up to 4 h irradiation was observed to be almost equal in the absence and presence of NaN_3. This implies that no $^1O_2$ is initially present in the system and the results suggest that $^1O_2$ begins to appear at photobleaching times longer than 4 h. Additional experiments with DABCO, which is another well known oxygen singlet quencher,[3,5] showed that DABCO had no effect at all on the initial rate of Orange II photobleaching by the O_2 in solution. After 4 h more readily oxidizable organic compounds predominate in solution as the concentration of Orange II (at pH 3) drops below 50% of the initial value. This point will be taken up again below. The decoloration of Orange II in solution was observed to be autocat-

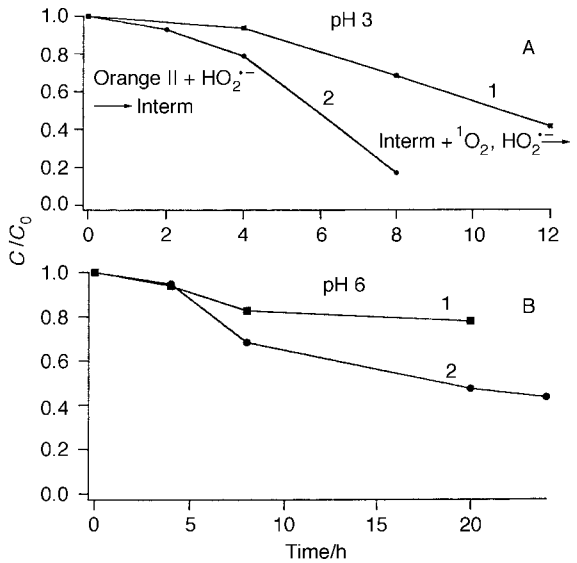

Fig. 1 Reduction in concentration of a 0.32 mM Orange II solution at (A) pH 3 and (B) pH 6 under light irradiation in the presence of NaN_3. Other experimental parameters are described in the text. In both frames trace 1 refers to solutions containing NaN_3 and trace 2 is in the absence of NaN_3.

alytic since the rate of Orange II disappearance accelerated during the photodegradation. To further test the nature of the radical intermediate generated in solution during the decoloration/degradation of Orange II, photolysis of Orange II was carried out in the presence of 1,4-benzoquinone (BQ), which is a known superoxide radical quencher *via* fast electron transfer.[16-18]

$$BQ + O_2^{-\cdot} \rightarrow BQ^{-\cdot} + O_2$$

(benzoquinone radical formation) (1)

The addition of millimolar concentrations of BQ to oxygenated Orange II was seen to preclude the photoinduced bleaching in acid or in basic media due to formation of O_2 and $BQ^{-\cdot}$ with a bimolecular rate of 9.6×10^8 M^{-1} s^{-1}.[19] This reaction is used to detect $O_2^{-\cdot}$. From the results presented in Fig. 1 when Orange II is irradiated in the presence of the $^1O_2$ scavanger NaN_3, it can be suggested that the superoxide radical anion is involved in Orange II (D) bleaching:

$$D^* + O_2 \rightarrow D^{+\cdot} + O_2^{-\cdot} \quad (2)$$

Since BQ precludes the photobleaching of Orange II, $O_2^{-\cdot}$ seems to be involved from the beginning in the decoloration of Orange II in Fig. 1. The photodegradation of Orange II generates compounds in solution at longer irradiation times that are susceptible to react with $^1O_2$. These species will be discussed in the Results and discussion section below. The active species during the decoloration up to 4 h at pH 3 is suggested to be $HO_2^{\cdot}$ in the equilibrium shown below:

$$HO_2^{\cdot} \rightleftharpoons O_2^{-\cdot} + H^+ \quad pK_a = 4.8 \quad (3)$$

The lack of photobleaching at pH 6.0 can be attributed to the fact that hydroperoxy radicals are not available in solution since the superoxide anion is not protonated at this pH.

Nature of the intermediates intervening in Orange II photobleaching as observed by fast kinetic spectroscopy

Fig. 2(A) presents the laser induced spectra for a solution of Orange II under an Ar atmosphere at different times after the laser pulse. The main feature of the spectra is seen to be the strong photobleaching of the band around 480 nm. This indicates that the intermediates formed after the laser pulse in solution absorb more weakly than Orange II in the spectral region between 450 and 550 nm. But the peak at 550 nm is attributed to the formation of Orange II radicals ($D^{+\cdot}$) in agreement with the assignment suggested by Vinogdopal and Kamat.[10] The bands are observed to be similar at different times after the laser pulse, giving evidence that only one species is responsible for the observed photobleaching. A weak absorption is observed at $\lambda \simeq 550$ nm decaying to zero in ≈ 1 μs. Also a narrow band is observed at $\lambda = 390$ nm, showing that further bleaching also occurs at other λ values.

Fig. 2(B) shows the spectra after the laser pulse for the solution used in Fig. 2(A) but under an O_2 atmosphere (1 bar). A significant difference in the laser induced spectra is noticed at $\lambda \simeq 550$ nm. An increase in the yield of Orange $II^{+\cdot}$ ($=D^{+\cdot}$) cation radicals is observed in oxygenated solutions relative to Ar saturated solutions. In air saturated solutions, the intensity of the $D^{+\cdot}$ peak at 550 nm was reduced in comparison to O_2 purged solutions but was greater than the signals observed in the case of Ar solutions.

Fig. 3(A) shows the concentration quenching induced after the laser pulse in Orange II Ar saturated solutions. The maximum of the photobleaching peak at 480 nm is taken to plot the data presented in Fig. 3(A). This figure shows that when the dye concentration was increased from 0.037 mM (6 ppm) to 0.15 mM (25 ppm) the decay rate becomes faster. A reduction in the photobleaching halflife $\tau_{1/2}$ from ≈ 0.2 μs to ≈ 0.05 ms is observed, as shown in the inset to Fig. 3(A), when the dye concentration in solution is increased from 0.037 mM to 0.15 mM. Fig. 3(B) presents similar decays for Orange II solutions but under O_2 (1 bar). The $\tau_{1/2}$ found in this latter case were ≈ 0.5 μs for the diluted solution and ≈ 0.1 μs for the

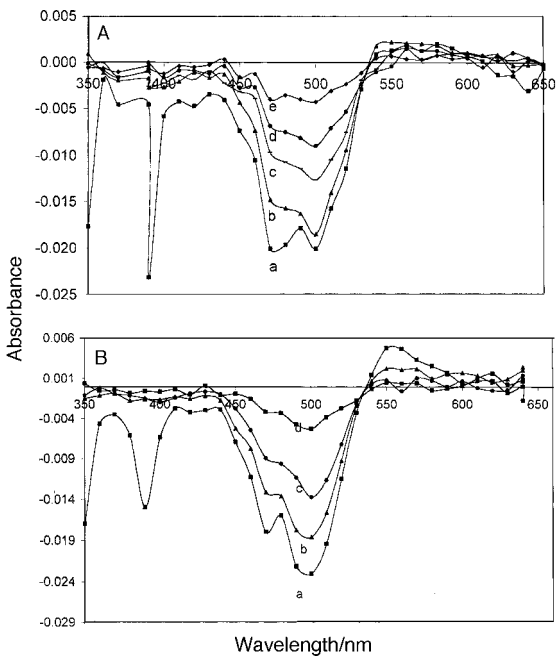

Fig. 2 (A) Laser induced spectroscopy of an Ar saturated Orange II (0.32 mM) solution at different times after the laser pulse: (*a*) 10^{-8}, (*b*) 3×10^{-7}, (*c*) 9×10^{-7}, (*d*) 5×10^{-7} and (*e*) 10^{-6} s. For further experimental details see text. (B) As in (A) but in an O_2 saturated solution: (*a*) 10^{-8}, (*b*) 10^{-7}, (*c*) 3×10^{-7} and (*d*) 10^{-6} s.

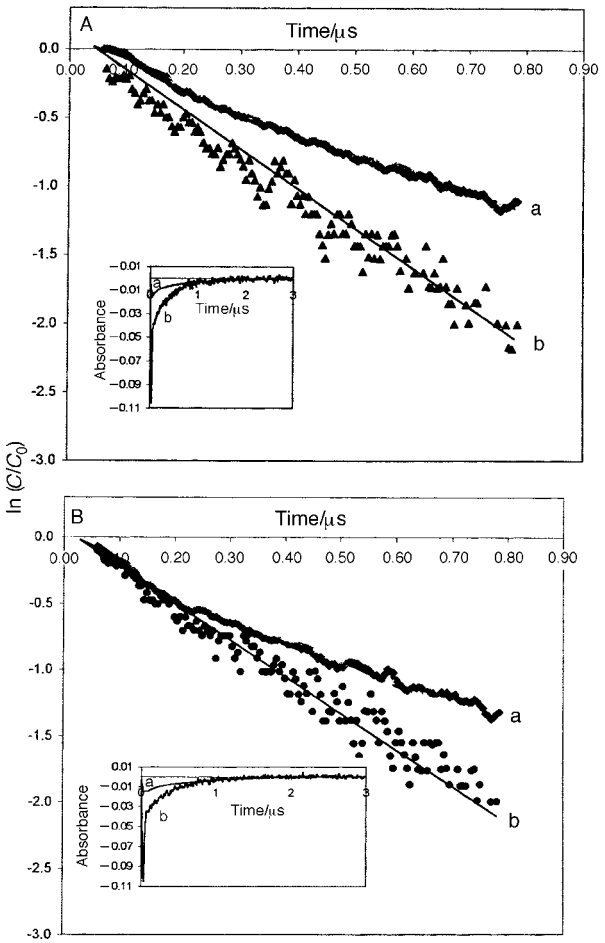

Fig. 3 Transient of Orange II: (*a*) 0.037 and (b) 0.15 mM in Ar purged solution. (B) Same as (A) with O_2 (1 bar). For more details of both insets see text.

more concentrated solution. The insets in Fig. 3(A) (trace a) and Fig. 3(B) (trace a) show a similar initial decay.

Vinogdopal and Kamat[10,11] have recently reported a lifetime for the Orange II (=D) excited state (D*) of $\approx 10^{-10}$ s and ascribed this state to the Orange II singlet. The results presented in Fig. 3 suggest the formation of Orange II aggregates in concentrated solutions. Dimer formation is indicated in eqn. (4)

$$D^* + D \rightarrow D_2^* \rightarrow D^{+\cdot} + D^{-\cdot} \quad (4)$$

since the decay times in Fig. 3 are seen to be different from the singlet lifetime of D*. The bleaching of Orange II would occur due to the ionization of Orange II, through the mechanism:[5,11]

$$D + nh\nu \rightarrow D^{+\cdot} + e^-(aq) \quad (5)$$

$$e^-(aq) + D \rightarrow D^{-\cdot} \quad (6)$$

The concentration quenching reported (Fig. 3) suggests intermediate dimers in solution

$$D + D \longrightarrow \text{dimer} \xrightarrow{h\nu}$$

$$(D^{+\cdot} + D^{-\cdot})_{\text{dimer g.s.}} \longrightarrow D^{+\cdot} + D^{-\cdot} \quad (7)$$

lead to the formation of the cation $D^{+\cdot}$ and anion $D^{-\cdot}$ radicals of Orange II. The value of n in eqn. (5) has been reported for Orange II to be ≈ 2.1[12] with excitation by a pulsed ruby laser. This is an indication for biphotonic ionization of Orange II proceeding through the formation of a dimer intermediate. If aggregates of the dye are present in solution the ionization and electron transfer will occur monophotonically with high efficiency.

Fig. 4 shows the absorption of cation radicals at 550 nm. This absorption is significantly higher in the presence of oxygen than in the case of Ar saturated solutions due to the increased radical formation in oxygenated media. The bleaching recovery in oxygenated solutions of Orange II [Fig. 4(A)] is seen to be faster than in Ar solutions [Fig. 4(B)] due

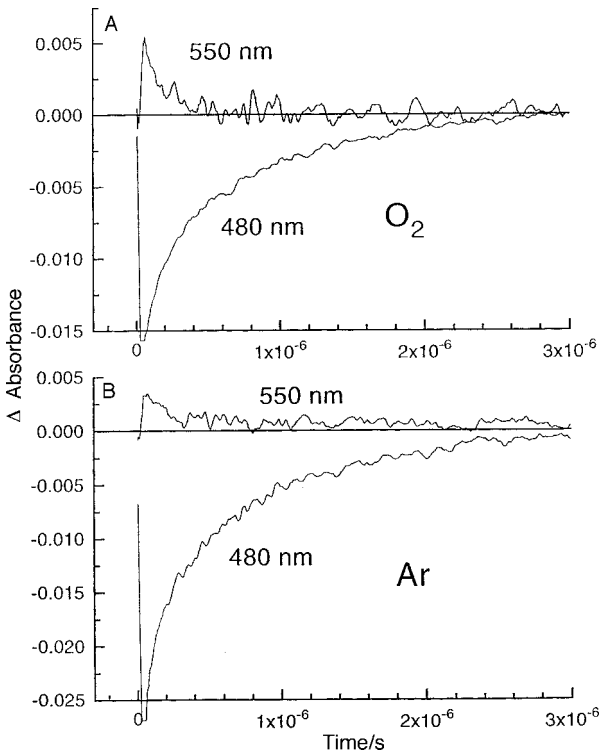

Fig. 4 Transient spectra of Orange II solutions as previously used in Fig. 3(A) in the presence of O_2 and (B) in the presence of Ar.

to the competition of reactions 8 and 9:

$$(D^{+\cdot} + D^{-\cdot})_{\text{dimer g.s.}} \rightarrow D + D \quad (8)$$

$$D^{-\cdot} + O_2 \rightarrow D + O_2^{-\cdot} \text{ (superoxide radical formation)} \quad (9)$$

Because after the laser pulse $[D^{+\cdot}] \approx [D^{-\cdot}]$, the removal of D^- due to the reaction with O_2 accounts for the residual bleaching at times >2 μs in the presence of O_2 in the inset of Fig. 3(B). Furthermore, the maximum intensity of the 550 nm band in Fig. 2 for $D^{+\cdot}$ is attained when the bleaching at 480 nm also attains a maximum. The optical density at 480 nm in Fig. 2 would be given by $\Delta = \varepsilon_D [D]_t + \varepsilon_{D^{+\cdot}} [D^{+\cdot}]_t + \varepsilon_{D^{-\cdot}} [D^{-\cdot}]_t - \varepsilon_D [D]_0$ where $[D]_0$ the concentration of the dye at any time t, is equivalent to the concentration of the dye at $t = 0$ before the pulse: $[D]_0 = [D]_t + [D^{+\cdot}]_t + [D^{-\cdot}]_t$. After 1 μs the absorbance at 550 nm disappears but a residual bleaching between 450 and 550 nm is still observed. This can only be due to an additional reaction taking place parallel to the reaction shown in eqn. (5).

The anion radical $D^{-\cdot}$ has been observed by Kamat and coworkers[9,10] below 400 nm, but in oxygenated solutions the anion radical $D^{-\cdot}$ was not observed due to the strong photobleaching signal present in this region. Reactions of anion radicals, as shown in eqn. (9) are well known regenerative mechanisms for many dyes and have been reported previously for xanthenes, oxazines[4] and porphyrins.[6] The O_2 in solution removes the $D^{-\cdot}$ anion radical, allowing the observation of $D^{+\cdot}$ besides leading to the formation of the superoxide radical in eqn. (9). However, the $D^{+\cdot}$ cation radical reacts by nucleophilic substitution and deactivates further with the formation of photoinduced intermediates.[2]

The intersystem crossing to Orange II(T_1) is known to be inefficient.[13,14] The latter process is not favored when competing with the deactivation channel $S_1 \rightarrow S_0$. The triplet quantum yield for Orange II has been reported to be[10] $\Phi T \approx 10^{-3}$. Since $S_1 \rightarrow S_0$ competes with $D^* + O_2$ the probability P_1 of the reaction $D^* + O_2 \rightarrow D^{+\cdot} + O_2^{-\cdot}$; leading to radical formation can be estimated from: $k[O_2]/(\tau^{-1} + k[O_2]) \approx 4.8 \times 10^{-4}$. This compares with the probability P_2 for the singlet deactivation channel $D(S) \rightarrow D$: $\tau^{-1}/(\tau^{-1} + k[O_2]) \approx 1$, with τ being the lifetime of the singlet (10^{-10} s), k the diffusion control rate for the reaction of D with O_2 in aqueous solution (9.6×10^9 M^{-1} s^{-1}) and the oxygen concentration $[O_2] \approx 0.5 \times 10^{-3}$ M. Only a very small fraction of the initial Orange II would lead to the formation of radicals $D^{+\cdot}$ and $D^{-\cdot}$. The latter observation further backs the stability of Orange II and its use as a textile dye.

A more pronounced quenching of the $D^{+\cdot}$ cation radical at 550 nm was observed in air than in solutions purged with Ar. But the reaction was slower than in O_2. This provides additional evidence for the formation of $O_2^{-\cdot}$ or $HO_2^{\cdot}$ in oxygenated solutions.

The photoproduction of H_2O_2 was observed only at pH < 4.5 since above this pH superoxide radical dismutation takes place. The radical $O_2^{-\cdot}$ at acidic pH subsequently reacts in solution[15]

$$O_2^{-\cdot} + H^+ \rightarrow HO_2^{\cdot} \text{ (dismutation)} \rightarrow H_2O_2$$

(radical recombination) (10)

Gas atmosphere and oxygen pressure effects on the photobleaching of Orange II under steady-state irradiation

Fig. 5 presents the decrease of Orange II concentration as a function of time in a Suntest solar light simulator. The decrease of the Orange II concentration was measured by the HPLC technique (see details in the Experimental section). Fig. 5 presents the effect of three different gases and the effect of the O_2 pressure on the disappearance of Orange II. The O_2 in solution in the dark did not have any effect on the Orange II

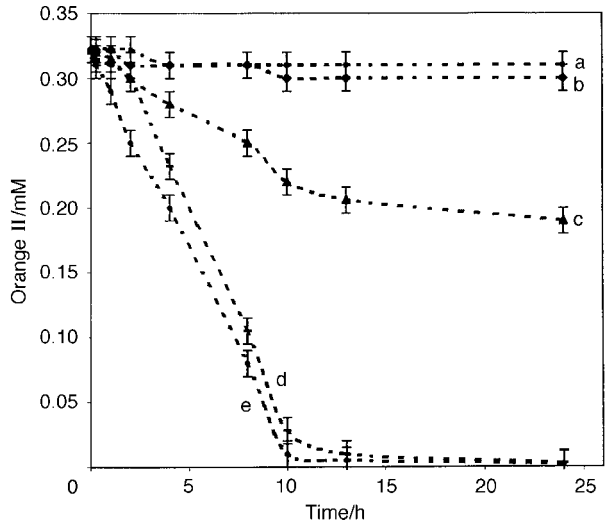

Fig. 5 Orange II disappearance as a function of time under different gas atmospheres in the dark and for light irradiated solutions at pH 3: (*a*) O_2 (1 bar), dark; (*b*) Ar (1 bar), light; (*c*) air (1 bar), light; (*d*) O_2 (1 bar), light; (*e*) O_2 (1.5 bar), light.

concentration within 24 h. The effect of light irradiation on solutions of Orange II with Ar is seen to be negligible. When air was used a 37% decrease of Orange II was observed within 24 h. Complete decoloration of Orange II is observed within 10 h for solutions containing O_2 (1.5 bars). The photochemical degradation with O_2 (1.5 bars) presented in Fig. 5 proceeds with zero order. The rate of the decrease in dye concentration does not change during the time of photodegradation. The data is fitted by the line $y = 0.31 - 0.034x$ with a correlation factor of 0.976. Pressures of 1.0 and 1.5 bars of O_2 led to slightly different degradation kinetics as reported by the results shown in Fig. 5. The solubility of O_2 in 0.032 mM Orange II solutions did not differ from the solubility reported for O_2 in pure water at 20 °C (0.0305 L L^{-1}).

The decoloration of the Orange II solutions in the presence of O_2 (1.0 bar) is kinetically faster than when air or Ar atmospheres were used. The decoloration is due to azo-bond breakage.[13,14]

The total organic carbon (TOC) for the solution in Fig. 5 was observed to be 10% lower than the carbon content normally expected for a 0.32 mM solution of this dye. The Orange II used was a hydrate. This hydration accounts for the disagreement observed between the added amount of Orange II and the effective TOC detected for the dye. The TOC decrease within 24 h in air (1 bar), O_2 (1 bar) and O_2 (1.5 bars) were: 8, 14 and 30%, respectively. These are significantly smaller than the Orange II disappearance reported in Fig. 5. This indicates the existence of long-lived intermediate(s) in solution

$$\text{Orange II} \xrightarrow{h\nu,\, O_2,\, \Sigma k_1} [\text{long-lived intermediates}] \xrightarrow{\Sigma k_2} CO_2 \quad (11)$$

The experimental results suggest that $\sum k_1$ has a much larger value than $\sum k_2$ due to the existence of long-lived intermediates generated during the degradation process. No appreciable reduction of the total TOC is therefore necessary to effectively remove the color from dye solutions. This is important for any application of the photobleaching approach as used in this study.

pH effects and concentration quenching during Orange II photobleaching

The photobleaching kinetics were observed to depend on the acidity of the medium since this is an important factor in determining the equilibrium of the dye species in solution.[20] The pH dependency indicates protonation and deprotonation

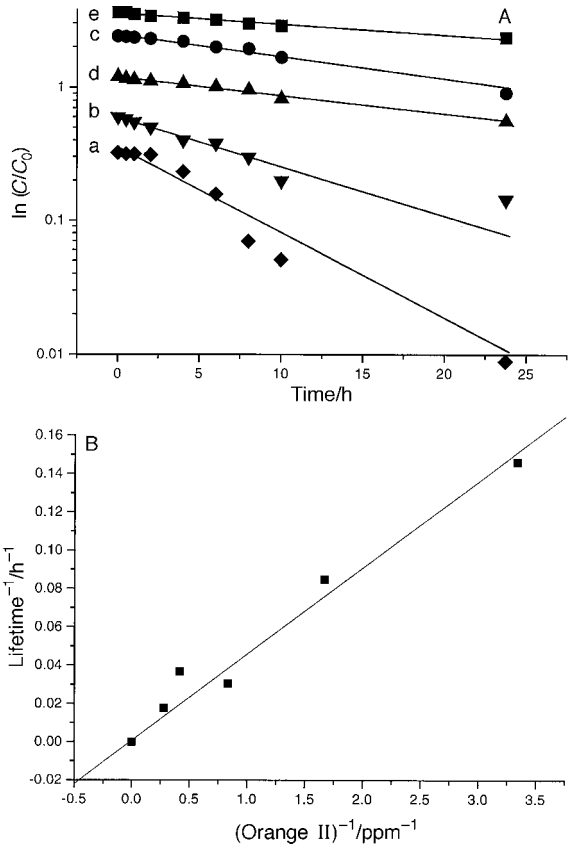

Fig. 6 (A) Logarithmic plot for concentrations of Orange II as function of time under Suntest irradiation: (*a*) 0.3, (*b*) 0.6, (*c*) 1.2, (*d*) 2.4 and (*e*) 3.6 mM. (B) Plot of the reciprocal of the photobleaching time under steady-state illumination as a function of reciprocal Orange II concentration for the dye concentrations in (A).

of the N atoms in Orange II as the pH of the solution is varied. This behavior is found in organic compounds containing hydrophobic and hydrophilic groups as is the case for Orange II.[21] The photodegradation kinetics for various Orange II concentrations were also investigated by the HPLC technique. As expected the disappearance of Orange II proceeded much more rapidly at lower concentrations (0.32 mM) than at the higher concentration (3.6 mM). In the latter case an intensely colored solution with a TOC of 672 ppm C is present in solution. The degradation proposed in this study is shown to work at TOC concentrations >20 times the concentrations found commonly for pollutants in water reservoirs.

Fig. 6(A) shows the logarithmic plot for the concentration of Orange II as a function of irradiation time. The decrease observed for each concentration could be fit to a pseudo first-order kinetics law:

$$C(t) = C_0 \exp(-kt) \quad (12)$$

The rate constants as a function of Orange II concentration are given in Table 1.

Fig. 6(B) shows the plot of the reciprocal of the photobleaching time as a function of the reciprocal dye concentration

Table 1 Rate constants observed for Orange II degradation in the presence of O_2 (1 bar)

Orange II concentration/mM	Rate constant/h^{-1}
0.32	0.1948
0.60	0.0591
1.20	0.0396
2.40	0.0311
3.60	0.0168

and presents the data of Fig. 6(A) in terms of concentration quenching. Eqns. (14)–(16) describe the quenching of the excited state (D*) as the concentration of Orange II (=D) increases, leading to dimer (D_2) and trimer (D_3) formation

$$D \xrightarrow{h\nu} D^* \quad (13)$$

$$D^* + D \rightarrow D_2^* \quad (14)$$

$$D^* + D \rightarrow D_2 \quad (15)$$

$$D_2^* + D \rightarrow D_3 \quad (16)$$

The straight line fit observed in Fig. 6(B) is explained by eqns. (17)–(20) below, where [D*] is the average concentration of excited state chromophore in the illuminated volume V, W is the number of photons absorbed in the illuminated volume V, τ is the lifetime of the excited state D*, k is the rate constant of the reaction of O_2 with Orange II and k' is a scaling factor between dye concentration and the absorbance per unit volume of dye.

$$[D^*] = \int \frac{[D^*]}{V}(r)\,dV \quad (17)$$

$$[D^*] = \frac{W}{k'[D]} + \left\{\frac{1}{\tau} + k[O_2]\right\} \quad (18)$$

If concentration quenching is the main deactivation channel of D* then

$$k'[D] \gg \frac{1}{\tau} + k[O_2] \quad (19)$$

and if all the incident light is absorbed by the dye in solution a further increase in the dye concentration does not lead to further absorption of light energy. In this case it is possible to write

$$[D] \approx \frac{W}{k'[D]} \quad (20)$$

because the degradation rate $\approx k$ [D] [oxid] and the dependence of the degradation rate *vs.* D is:

$$k \text{ (degradation rate)} = \frac{1}{[D]} \quad (21)$$

The treatment of the data shows that the degradation is inversely proportional to the Orange II concentration [Fig. 6(B)].

Orange II has been reported to exist in different structures in solution. Due to the hydrophobic/hydrophilic character of Orange II, this dye forms a defined proportion of monomers, dimers, trimers and higher aggregates as a function of concentration and solution pH.[14] The structures of these aggregates in solution have been described in the literature for fluorescein,[4] porphyrins,[6] methylene blue[15] and eosin.[21,22]

Intermediates observed during Orange II photodegradation and H_2O_2 photoproduction

Fig. 7 presents Orange II photobleaching intermediates in solution as a function of time as determined by HPLC. After 2 h of light irradiation, 4-hydroxybenzenesulfonic acid, 1,2-naphthol and 1,2-naphthoquinone were detected as photoproducts. After 24 h, the products in solution are: oxalic acid (86%), 4-hydroxybenzenesulfonic acid (6%), acetic acid ($\approx$3%), 1,3-isobenzofurandione ($\approx$2%), formic acid ($\approx$2%) and 4-hydroxyglyoxalic acid ($\approx$1 %). Orange II is seen to practically disappear in solution after 10 h irradiation. The evolution of the photobleaching products are shown in Scheme 1.

The reaction of O_2 with 4-hydroxybenzenesulfonic singlet acid in Scheme 1 is the key reaction leading to $^1O_2$. The time

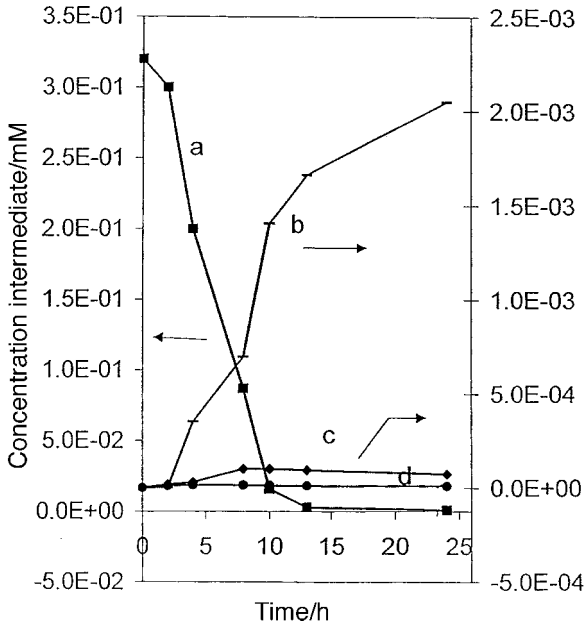

Fig. 7 Most important photobleaching intermediates observed by HPLC during Orange II photodegradation as a function of time. (*a*) Orange II, (*b*) oxalic acid, (*c*) 4-hydroxybenzenesulfonic acid and (*d*) acetic acid.

evolution of this intermediate in Fig. 7 indicates that it may be the key aromatic intermediate (besides the 1,3-isobenzofurandione formed in smaller amounts). It has a singlet lifetime of $\approx$30 ns and reacts with O_2, leading to $^1O_2$, after the initial reaction stages. The other two intermediates, oxalic and acetic acid, do not absorb visible light and therefore do not lead to $^1O_2$. Once $^1O_2$ is generated in solution it further promotes dye degradation as shown previously in Fig. 1(A).

Fig. 8 presents the generation of H_2O_2 with time for Orange II solutions at pH 3 having O_2 concentrations of 1 or 1.5 bars. Lower concentrations (of H_2O_2) were observed at pH values of 5 and 6 (not shown in Fig. 8). Therefore, production of H_2O_2 is possible when Orange II and O_2 react in solution under light irradiation. The peroxide formed in the solution was detected using Merkoquant® paper. At times less than 5 h a deep orange color was observed due to the azo dye in solution. This precluded a quantitative determination of the characteristic blue color due to the peroxide. Iodometric or Ce^{4+} titration could not be applied for the quantitative determination of the H_2O_2 in solution. The strong coloration of the solution due to the Orange II in the initial stages of the reaction did not allow the use of spectrophotometric detection methods either. An additional technique tried for the detection of H_2O_2 involved dimerization of *p*-hydroxyphenylacetic acid (POPHA).[23,24] In the presence of H_2O_2 and with added horseradish peroxidase a fluorescence peak (at 400 nm excitation at 315 nm) is observed and indicates that the peroxide is present, due to its reaction with the acid.

As seen from Figs. 7 and 8, Orange II itself, and not the more biodegradable intermediates, has to be present in solution to interact with O_2 and photoproduce H_2O_2. The peroxide concentration attains its maximum value after $\approx$10 h and decreases at longer times due to oxidation of the degradation intermediates. Peroxide formation is due to direct electron transfer from the dye to O_2, and is the precursor of the observed peroxides as described in eqns. (22) and (23). The intermediates of Orange II degradation are not able to participate in the photoproduction of H_2O_2. Peroxide formation is therefore possible only as long as the dye is still present in the solution. The shape of the curves shown in Fig. 8 shows that the intermediates formed in solution, once present in meaningful amounts, do not lead to peroxides.

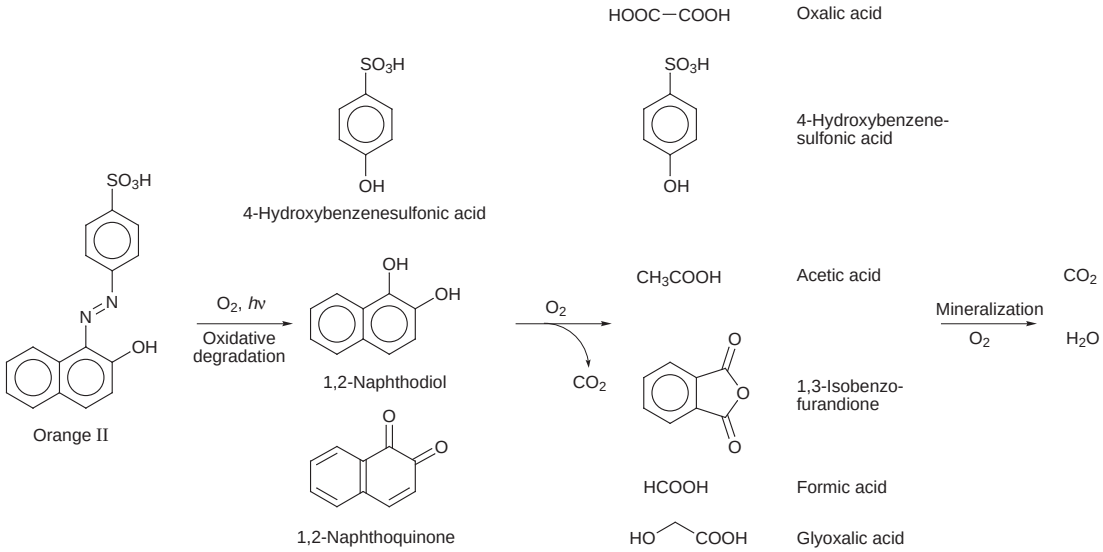

Scheme 1

The mechanism leading to peroxide formation in solution involves eqns. (22) and (23). It is known that the quantum yield for the formation of Orange II(T_1) triplet upon light irradiation is very low.[10–15] The electron transfer from Orange II (=D) to O_2 would then proceed as follows:

$$D \xrightarrow{h\nu} D^* \xrightarrow{O_2} D^{+\cdot} + O_2^{-\cdot} \quad (22)$$

$$O_2^{-\cdot} + H^+ \rightarrow HO_2^{\cdot} \rightarrow H_2O_2 + O_2 \quad (23)$$

Since the pK_a of $HO_2^{-\cdot}$ is 4.8 ± 0.1,[20] the participation of $HO_2^{\cdot}$ in eqn. (23) in H_2O_2 formation below pH 4.8 would proceed favorably, as was observed during this study.

On thermodynamic grounds, charge transfer from Orange II in the excited state (D*) to O_2 is possible leading to Orange II degradation (Fig. 7) and H_2O_2 photoproduction (Fig. 8). In contrast, charge transfer from the Orange II ground state to O_2 is not possible in the dark (Scheme 2). By cyclic voltammetry (see Experimental section) the oxidation potential of Orange II was measured and found to be 0.76 V (NHE). The low energy edge from the absorption of Orange II was found at $\lambda \approx 565$ nm or 2.3 eV. This is the transition energy of one electron to the excited state for Orange II. If ΔG° is the energy gap between the ground state and excited state D* from which oxidation occurs, the reduction potential of Orange II* can be estimated through the relation[25]

$$\Delta E^\circ(D^+/D^*)(V) = E^\circ(D^+/D)(V) - \Delta G^\circ(D^*/D)(eV) \quad (24)$$

Inserting the values of 0.76 V and 2.3 eV into the right hand side of eqn. (24), a value of −1.54 V (NHE) is found for the excited state standard reduction potential of the azo dye. This potential for the couple O_2/O_2^- has a value of −0.16 V *vs.* NHE[20] (Scheme 2).

The sulfate anion evolution during the photobleaching of Orange II has been followed as a function of time by ion liquid chromatography (ILC, see Experimental section). The acid catalyzed nucleophilic substitution leading to hydrolysis of Orange II and 4-hyroxybenzenosulfonic acid was accompanied by sulfate release into solution in a three-stage process showing the following kinetics: (*a*) within 2 h about 20% sulfate was released in a relatively quick process, (*b*) up to 15 h about 30% of the sulfate was seen to appear with slower kinetics and finally (*c*) during the following 7 h the remaining fraction of ≈40% was generated with a significantly faster kinetics than in (*b*).

Nitrates and nitrites from the Orange II azo linkage were not detected in solution. In acid solution (pH ≈3) the NH_4^+ ion was found with a concentration equivalent to about 20% of the total stoichiometric content of N in the solution. Shorter chain nitroaliphatics formed at later stages during the photobleaching could not be unambiguously identified by HPLC techniques. No adequate available reference substances—commercial or not—were found for this analysis.

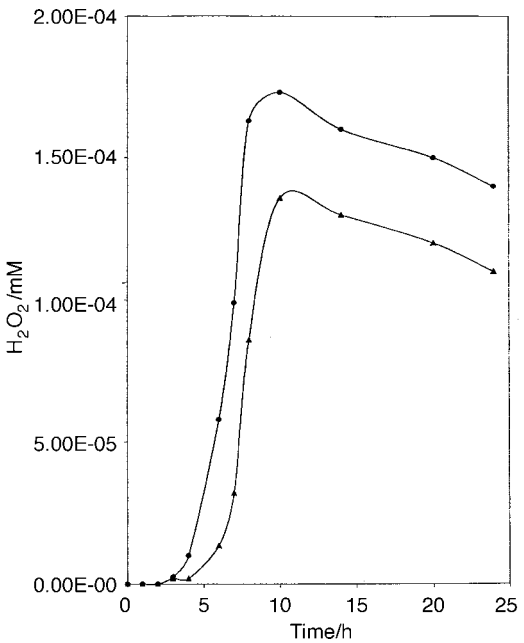

Fig. 8 Photogeneration of H_2O_2 as a function of time for a solution of Orange II (0.32 mM) in a Suntest irradiator and O_2 pressures of (*a*) 1 and (*b*) 1.5 bars.

Photobleaching as an effective pretreatment prior to biological degradation

Solutions of Orange II (0.32 mM), were pretreated by irradiation under visible light for 10 h in the presence of O_2 (1 bar).

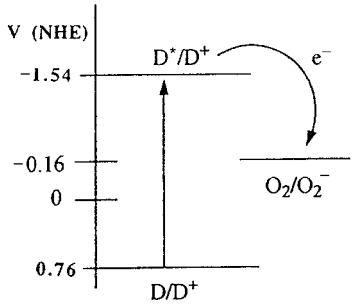

Scheme 2

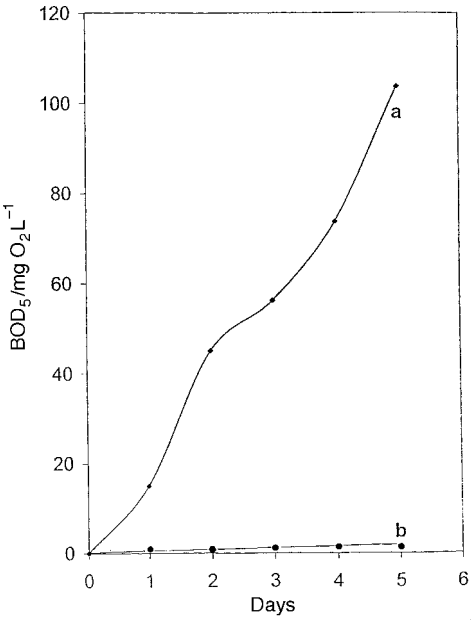

Fig. 9 (*a*) BOD_5 for an Orange II (0.32 mM) solution photobleached for 10 h in a Suntest lamp; (*b*) shows the BOD_5 for a solution of Orange II not photobleached as in (*a*).

With this pretreatment the nonbiodegradable Orange II is practically removed from the solution as shown by Fig. 7, trace *a*.

The BOD_5 results are shown in Fig. 9, calculated using the following formula:

$$BOD_5 = \frac{BOD_{meas} - 0.01\{\%\text{inoculum} \times BOD_{inoculum}\}}{0.01 \times \{100 - \%\text{ inoculum}\}} \quad (25)$$

A steep rise of the BOD_5 curve is observed with time. The photobleaching in the solution generates intermediates with more oxidized functional groups than the initial Orange II (see Scheme 1), which account for the steep rise of the BOD values. The BOD values are observed to increase from the very beginning showing the beneficial effect of the photobleaching. Fig. 9 also suggests that other non-biodegradable intermediates besides Orange II are removed from solution by the pretreatment used.

Conclusions

The decoloration of Orange II has been studied by laser fast kinetic spectroscopy (high light fluxes) and by steady-state simulated solar visible light irradiation (low light fluxes). Oxygen is shown to enhance the formation of anion and cation radical species. The photobleaching is shown to be dependent on the pH, concentration of the dye and the gas atmosphere present over the solution. Experimental proof is provided for the participation of radical species during Orange II decoloration. Insight into the mechanism of Orange II decoloration is obtained and is based on laser spectroscopy, UV-vis spectrophotometry, HPLC, TOC and BOD data. Visible light-induced bleaching of Orange II produces a loss of absorbance (color), CO_2 evolution and the generation of long-lived intermediates in solution. Orange II (0.32 mM) can be completely bleached under visible light irradiation in about 13 h with O_2 (1 bar). The six most important degradation products due to photobleaching in oxygenated solutions have been identified by HPLC. Oxalic acid was the main degradation product accounting for about 86% of the total. The bleaching decreased significantly at higher concentrations of Orange II. Peroxide formation during Orange II photobleaching was unambiguously identified. The potential measured for Orange II suggested that excited Orange II interacts with O_2 in solution leading to the formation of the azo dye cation with concomitant reduction of O_2.

Acknowledgements

This work was supported by the E.U. Environmental Program N° ENV-CT95-0064 (OFES N° 96.350).

Notes and references

1 G. Helz, R. Zepp and D. Crosby, *Aquatic and Surface Chemistry*, Lewis Publishing Company, Boca Raton, FL, 1995.
2 P. Pitter and P. Chudoba, *Biodegradability of Organic Substances in the Aquatic Environment*, CRC Press, Boca Raton, FL, 1990.
3 M. Hoffmann, M. Martin, W. Choi and D. Bahnemann, *Chem. Rev.*, 1995, **95**, 69.
4 H. Zollinger, *Color Chemistry*: *Synthesis, Properties and Applications of Organic Dyes and Pigments*, VCH Publishers, New York, 1987.
5 R. Rotomskis, S. Bagdonas and G. Streckyte, *J. Photochem. Photobiol, A.*, 1996, **33**, 61.
6 F. R. Hopf and D. G. Whitten, in *Porphyrins and Metalloporphyrins*, ed. K. M. Smith. Elsevier, Amsterdam, 1975, p. 667.
7 V. Naguib, C. Steel, S. Cohen and A. Young, *J. Photochem. Photobiol., A.*, 1996, **96**, 149.
8 D. Higgins and F. Barbara, *J. Phys. Chem.*, 1995, **99**, 3.
9 K. Vignodopal, D. Winkoop and P. V. Kamat, *Environ. Sci. Technol.*, 1996, **30**, 1660.
10 K. Vinogdopal and P. Kamat, *J. Photochem, Photobiol., A.*, 1994, **10**, 1767
11 K. Vinogdopal and P. Kamat, *Environ. Sci. Technol.*, 1995, **29**, 841.
12 V. Nadtochenko and J. Kiwi, *J. Chem. Soc., Faraday Trans.*, 1997, **93**, 2373.
13 C. Morrison, J. Bandara and J. Kiwi, *J. Adv. Oxid. Technol.*, 1996, **1**, 160.
14 J. Bandara, C. Morrison, J. Kiwi and C. Pulgarin. *J. Photochem. Photobiol., A.*, 1996, **99**, 57.
15 M. Halmann, *Photodegradation of Water Pollutants*, CRC Press, Boca Raton, FL, 1996, ch. 5.
16 B. H. J. Bielski and A. O. Allen, *J. Phys . Chem.*, 1977, **81**, 1058.
17 C. Plato and M. A. J. Rodgers, *Photochem. Photobiol.*, 1987, **45**, 79.
18 B. Patal and L. Wilson, *J. Chem Soc., Faraday Trans.*, 1972, **69**, 814.
19 R. Battino and L. Clever, *Chem. Rev.*, 1966, **66**, 395.
20 J. Edwards and R. Curci, in *Catalytic Oxidations with Hydrogen Peroxide as Oxidant*, ed. Kluwer Academic Press, Dordrecht, 1992, ch. 4.
21 A. Jaffe and H. Freeman, *Environmental Chemistry of Dyes and Pigments*, Wiley Interscience, New York, 1996, p. 61.
22 J. Kasche, *Photochem. Photobiol.*, 1967, **6**, 643.
23 C. Pulgarin and J. Kiwi, *Chimia*, 1996, **50**, 50 and refs. therein.
24 G. Guibault, P. Brignac and M. Jumeau, *Anal. Chem.*, 1968, **40**, 1256.
25 J. P. Scott and D. F. Ollis, *Environ. Prog.*, 1995, **14**, 88.

Paper 9/02425E